Accepted Manuscript

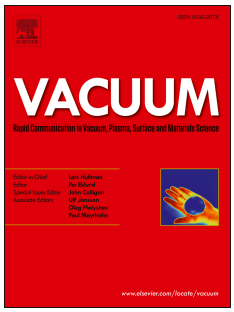

Effect of weld parameters on porosity formation in electron beam welded Zircaloy-4 joints: X-ray tomography study

Bharath Bandi, Soumitra Kumar Dinda, Jyotirmaya Kar, Gour Gopal Roy, Prakash Srirangam

PII: S0042-207X(18)31259-4

DOI: 10.1016/j.vacuum.2018.09.060

Reference: VAC 8273

To appear in: *Vacuum*

Received Date: 17 July 2018

Revised Date: 28 September 2018

Accepted Date: 29 September 2018

Please cite this article as: Bandi B, Dinda SK, Kar J, Roy GG, Srirangam P, Effect of weld parameters on porosity formation in electron beam welded Zircaloy-4 joints: X-ray tomography study, *Vacuum* (2018), doi: https://doi.org/10.1016/j.vacuum.2018.09.060.

Effect of weld parameters on porosity formation in Electron Beam Welded Zircaloy-4 Joints: X-ray tomography study

Bharath Bandi[1], Soumitra Kumar Dinda[1], JyotirmayaKar[1], Gour Gopal Roy[1], Prakash Srirangam[2].

[1] Department of Metallurgical and Materials Engineering, Indian Institute of Technology-Kharagpur, India.

[2]Warwick Manufacturing Group (WMG), University of Warwick, Coventry, CV4 7AL, UK

***Corresponding author email:** p.srirangam@warwick.ac.uk

Abstract:

Zircaloy-4 to Zircaloy-4 (Zr-4) similar butt joints were prepared using Electron Beam Welding (EBW) technique under different weld conditions such as with beam oscillation, without beam oscillation and at different welding speeds. Three-dimensional (3D) visualization of porosity in weld joints was carried out using X-ray computed tomography (XCT) technique. Quantification of porosity such as the average size, number and shape of the pores were evaluated and compared among weld joints produced under different conditions. XCT results show that the porosity of the welds increased substantially with the increase in the weld speed. More interestingly, the results also show that there is a significant decrease in porosity of the joint produced with beam oscillation condition. An increase in weld speed from 700 mm/min to 1000 mm/min resulted in a significant increase in pore density (from 16 to 313 per mm3) and it was observed that the average size of the macro pores increased from 96.4 µm to 121.5 µm. The joints prepared with beam oscillation produced least number of pores with minimum percentage of macro pores and maximum percentage of spherical pores in it. Raman spectroscopy results confirmed the presence of hydrogen gas in pores of all the weld joints.

Keywords: Zircaloy-4, Electron beam welding (EBW), Beam Oscillation, X-ray computed tomography (XCT), Porosity.

1. Introduction

Zircaloy-4 (Zr-4) is widely used as a structural material for containing radioactive fuel pellets in nuclear industries due to its low thermal neutron absorption cross section, excellent corrosion resistance, irradiation stability, and mechanical properties [1]. Owing to its excellent corrosion resistance, Zr-4 is also used as dissolver assemblies, heat exchangers etc in fast breeder reactor reprocessing plants [2]. In nuclear reactors Zr-4 is used to make components like fuel claddings, pressure tubes, and spacer grid assembly materials [3,4,5]. Zr-4 cladding with fuel pellets have to be sealed at both ends by welding end of the tubes to end caps and these weld joints should be strong enough to contain the fuel pellets during operating conditions [6]. The main requirements for the weld joints in the spacer grid assembly is to have minimum weld bead size to resist wear to nuclear fuel rods, and have maximum penetration of weld to meet the required mechanical strength such that it can effectively provide vertical and horizontal support to the fuel rods [7,8,9]. In all above applications, the strength and durability of Zr-4 to Zr-4 welds are very crucial for safe and smooth functioning of nuclear industries. More importantly, to produce a weld joint with a narrow weld bead size at a particular amount of weld penetration, a welding technique with high power density must be employed. In comparison to other conventional fusion arc welding processes, electron beam welding (EBW) is an effective welding technique as it offers advantages such as high power density, high depth to width ratio, high penetration, low heat input, small heat affected zone (HAZ) etc. [10,11,12].

The complex heating and cooling cycles associated with welding process often lead to formation of weld defects such as porosity, worm holes, cracks, incomplete fusion etc. [13,14,15,16]. Despite high vacuum conditions (in the level of 10^{-5} mbar), chances of porosity formation is possible even in EBW process [17,18]. For instance, Parga et al. studied

the mechanical properties of EB-welded Zr-4 sheets and observed porosity in the weld joints [19]. Moreover, this porosity formation greatly affects the mechanical and corrosion properties of weld joints. For instance Mishra et al. studied the effect of end plug weld defect on the operation of nuclear reactor and observed that the weld defect lead to extensive fuel reconstructing, fuel oxidation, cladding oxidation and hydride blister formation [20]. Similarly, Tao et al. found that the crack initiation during the tensile tests of laser spot welded Zr-4 spacer grid assembly started at gas pores in the weld region[21]. Hence, it is apparent from the literature that the formation of weld defects in Zr-4 joints is one of the major problems in nuclear industries. For this reason a proper understanding with detailed quantification of weld defects with respect to various weld parameters is crucial. In the past, various researchers have used X-ray computed tomography (XCT) technique to understand these weld defects. Nomoto et al. studied the porosity formation in various laser-welded samples using XCT technique and found that the tensile properties were greatly deteriorated by porosity in the welds [22]. Using XCT technique, Kar et al. recently concluded that the application of beam oscillation reduced the porosity content in EB-welded copper-304stainless steel joints [23]. Similar decrease in porosity content with the application of beam oscillation is seen by Dinda et al. in the EB welded steel – Fe Al alloy [17]. In this study along with the effect of beam oscillation, effect of weld speed on porosity formation in EB welded Zr-4 joints is studied. This is necessary because the increase in weld speed generally leads to finer microstructure and consequently better mechanical properties because of faster cooling rates. However, the mechanical properties of the joints are also dependent on porosity formation which can be influenced by weld parameters like weld speed and beam oscillation.

From the past research work, it is evident that the porosity formation in the Zr-4 weld joints could lead to catastrophic failures in nuclear industries. Hence, it is essential to study porosity

formation not only to optimize weld parameters, but also to improve the mechanical properties and structural integrity of the materials. In this publication, we used X-ray tomography study for the first time for 3D visualisation and quantification of porosity in EB welded Zr-4 joints under different weld conditions.

2. Experimental Procedure

2.1 Materials

Zircaloy-4 plates of 4 mm thickness were procured from Nuclear Fuel Complex (NFC), Hyderabad, India. As received sheets were analysed by X-ray spectroscopy for chemical analysis. Table 1 represents the chemical composition of Zr-4 plates. As received sheets were cut into plates of dimensions 100 mm x 50 mm x 4 mm and then polished with 320-grit emery paper. Prior to welding, plates were cleaned with acetone and placed into the welding fixtures along the longitudinal direction in a butt joint position.

Table 1: Chemical composition (by weight percentage)

Elements	Sn	Cr	Ni	Fe	Nb	Zr
Weight %	1.4	0.1	<0.005	0.23	0.1	98.17

2.2 Electron Beam Welding

Joining of Zircaloy-4 plates was carried out using 80 kV-12kW Electron Beam Welding machine at Indian Institute of Technology (IIT) Kharagpur, India. The power input of the electron beam was optimised to obtain full penetration on the Zr-4 plate. After obtaining complete penetration at a lowest possible power input, joints were prepared at four different parameters. Table 2 represents the weld parameters used in this study. To study the effect of beam oscillation, the oscillating beam was used for weld speed 1000 mm/min. Table 3 represents the weld variables used in this study.

Table 2: EBW process parameters used in this study.

Joint No	Voltage (kV)	Beam Current (mA)	Welding Speed (mm/min)	Oscillation Frequency (Hz)	Oscillation Diameter (mm)
1	70	42	700	Not used	Not used
2	70	42	900	Not used	Not used
3	70	42	1000	Not used	Not used
4	70	42	1000	300	0.5

Table 3: EBW weld process parameters.

Gun Sample Distance (mm)	**660**	**Filler Metal**	**None**
Number of pass	1	Gun Chamber Vacuum (mbar)	$<3 \times 10^{-5}$
Beam Focus Point (mm)	0	Work Chamber Vacuum (mbar)	$<1 \times 10^{-6}$

2.3 X-ray computed tomography (XCT)

X-ray computed tomography (XCT) studies were performed using a phoenix nanotom computed tomography (GE-Phoenix® model: V/TOME/XS) with 180 kV high-power Nano-focus tube with the sub-micron range in voxel size. This enabled 3D visualisation of the welds and quantification of porosity in the joints.

The weld samples were cut into 10 mm x 4 mm x 4 mm dimensions such that the cut pieces have fusion zone (FZ), HAZ and base metal in the XCT scan region in them. These cuts are taken from the centre of the weld samples such that the inhomogeneity in the weld beam which occurs at the ends of the welding samples will be avoided. A schematic representation of weld sample with the cut position of the XCT sample is shown in Figure 1. Samples were polished and cleaned with acetone. This sample was placed on a rotating platform between X-ray source and the detector and when X-rays pass though this sample a distinct grey scale radiograph is produced on the detector screen. The sample was placed in such a way that the weld was in the centre of the field of view of X- ray machine. The source and detector were adjusted to achieve maximum magnification; with additional magnification achieved from 4x

objective the combined resolution resulted to be 1.6µm. Numerous radiographic projections were taken throughout the 360^0 of the sample and back projected to reconstruct the virtual 3D volume of it. This volume consists of an array of pixels called voxels with an associated grey value between 0 and 65535 proportional to the relative attenuation/absorption of the x-rays by the material. Table 4 shows the parameters used in the XCT scans.

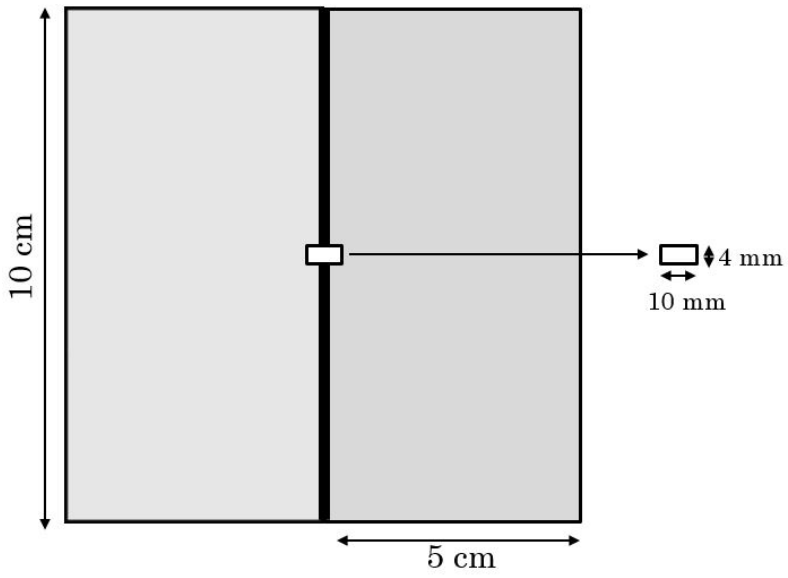

Figure 1: Schematic representation of weld sample and the corresponding position of XCT sample.

Table 4: XCT process parameters used in this study.

Parameters	Values
Voltage (kV)	150
Current (µA)	60
Timing (ms)	500
Filter (Cu-mm)	0.5
Number of Projections	1800
FOD (mm)	39.5
FDD (mm)	812.9

2.4 Raman Spectroscopy:

Raman spectroscopy technique was used to identify the entrapped gases in the heat-affected zones (HAZ) and fusion zones of all the four joints. The significant advancement of laser and photon detector technology in recent times made Raman spectroscopy a prominent technique in analysing gases present in the materials [24]. For this analysis, joints were cut into rectangular pieces of dimensions of 4 x 4 x 2 mm^3 from welded samples, polished by fine emery paper and cleaned with acetone. Raman spectroscopy machine details and process parameters used as listed in Table 5 below.

Table 5: Raman Spectroscopy machine details and process parameters.

Excitation Source	Argon-krypton mixed ion gas laser (wavelength 514 nm)
Spectrometer	Model T64000, Argon-krypton Laser)
Detector	Thermoelectric cooled front illuminated 1024 256 CCD.
Collection optics	Optical Microscope Model BX41
Focal Length (mm)	620
Frequency (cm-1)	100
Step size (nm)	0.0007
Grating (grooves/mm)	1800

3. Results and Discussion

The macrographs of the etched samples of all the joints is shown in Figure 2. It is observed that the length of fusion zone, heat affected zone and undercut decreased with increase in the weld speed of the joints. This is due to the fact that, as the welding speed decreases the electron beam stays on the specimen for a longer time. So, this increases the heat input into the specimen, which in turn increases the fusion zone and heat affected zone. Also at a given welding speed the oscillation beam condition will always have lesser heat input per unit length than that of the non-oscillation beam condition. This is due to the fact that during

oscillation beam condition the electron beam travels more distance per unit time. Because of this the fusion zone, heat affected zone and undercut for oscillation samples was found to be less than the non- oscillation samples.

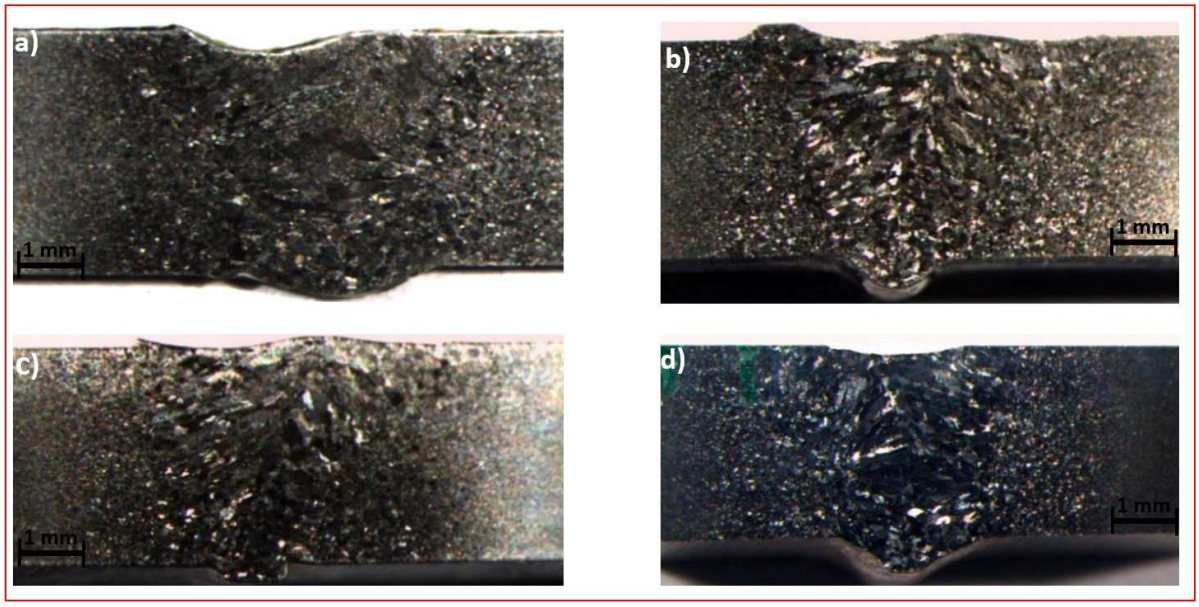

Figure 2: Macrographs of the weld samples: a) Joint 1, b) Joint 2, c) Joint 3, and d) Joint 4.

The optical micrographs shown in Figure 3 reveal the presence of porosity in the FZ's of all the joints. These images also suggests that the number of pores in the FZ increased with increase in weld speed and decreased with the application of beam oscillation. However, this inference cannot be taken as true for the whole joint, as these images only represent a tiny portion of the complete joints and can be easily misrepresented just by selecting different portions in the same joint. Moreover, the size and shape quantifications of the pores cannot be done in a systematic and reliable way using these 2D images. Figure 3 e) also shows the presence of porosity in the base metal, although it was very rarely found in insignificant levels.

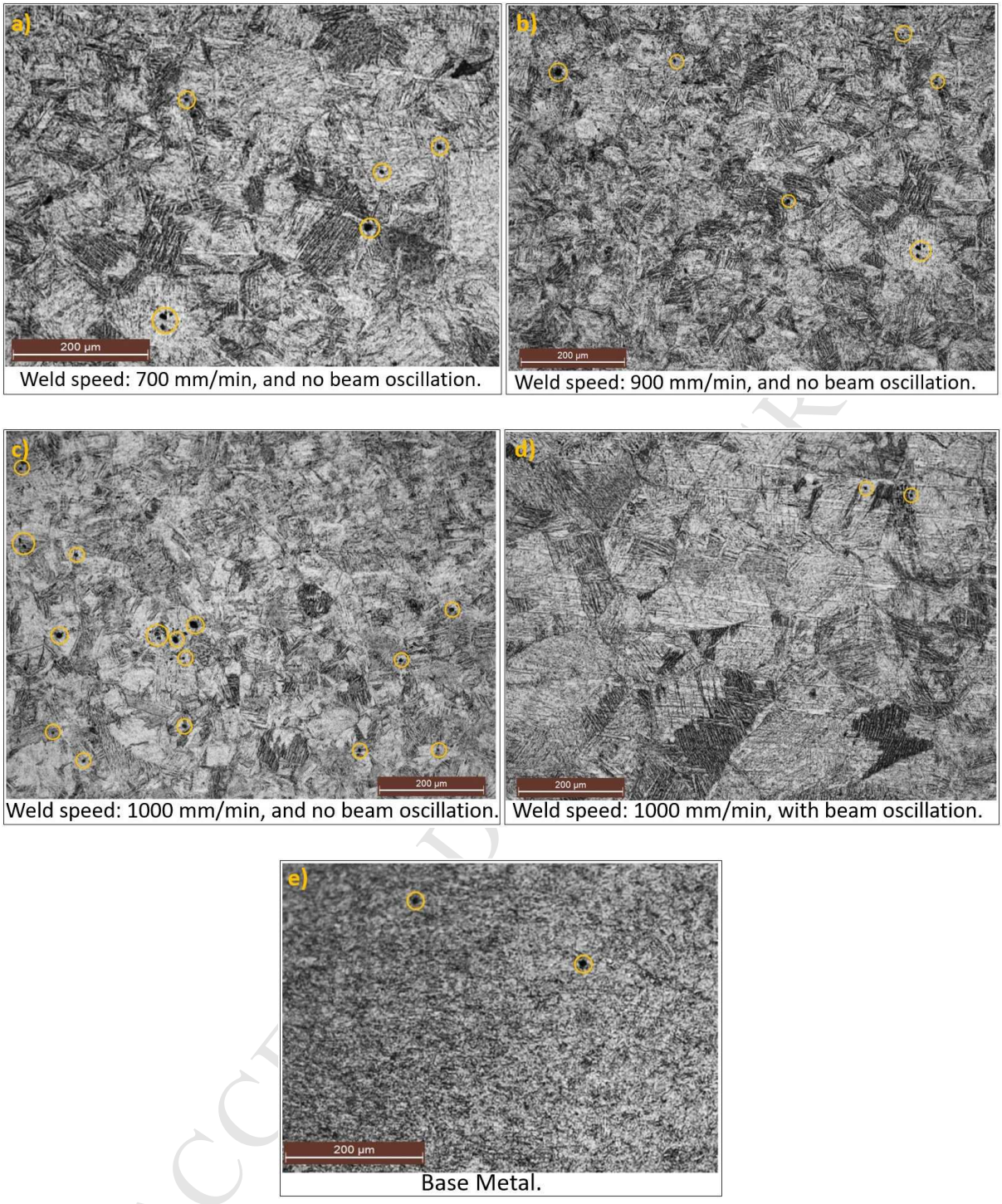

Figure 3: Optical micrographs showing pores in a). Joint 1 (FZ), b). Joint 2 (FZ), c) Joint 3 (FZ), d). Joint 4 (FZ), and e) Base metal.

Figure 4 shows the 3D reconstructed porosity distribution in Zr-4 joints for different weld conditions. Due to the obvious density difference between the matrix (Zircaloy-4) and pores, the 3D reconstructed images produced by XCT shows a clear contrast between pores and the

matrix. In case of without beam oscillation, porosity was found to increase with increase in weld speed as represented in figure 4 (a) to 4(c). Higher the weld speed, higher the cooling rate which results in entrapment of gases in the matrix. However, it is evident from Figure 4 (d) that the application of beam oscillation resulted in less porosity as compared to without beam oscillation. The main reason for this significant decrease in porosity with beam oscillation is due to the improved churning action in the molten pool, and also due to the repeated melting of the same spot in the weld track. It should be noted that even though there is some porosity visible in the base metal of some joints, it has been carefully removed from the actual quantification calculations discussed below.

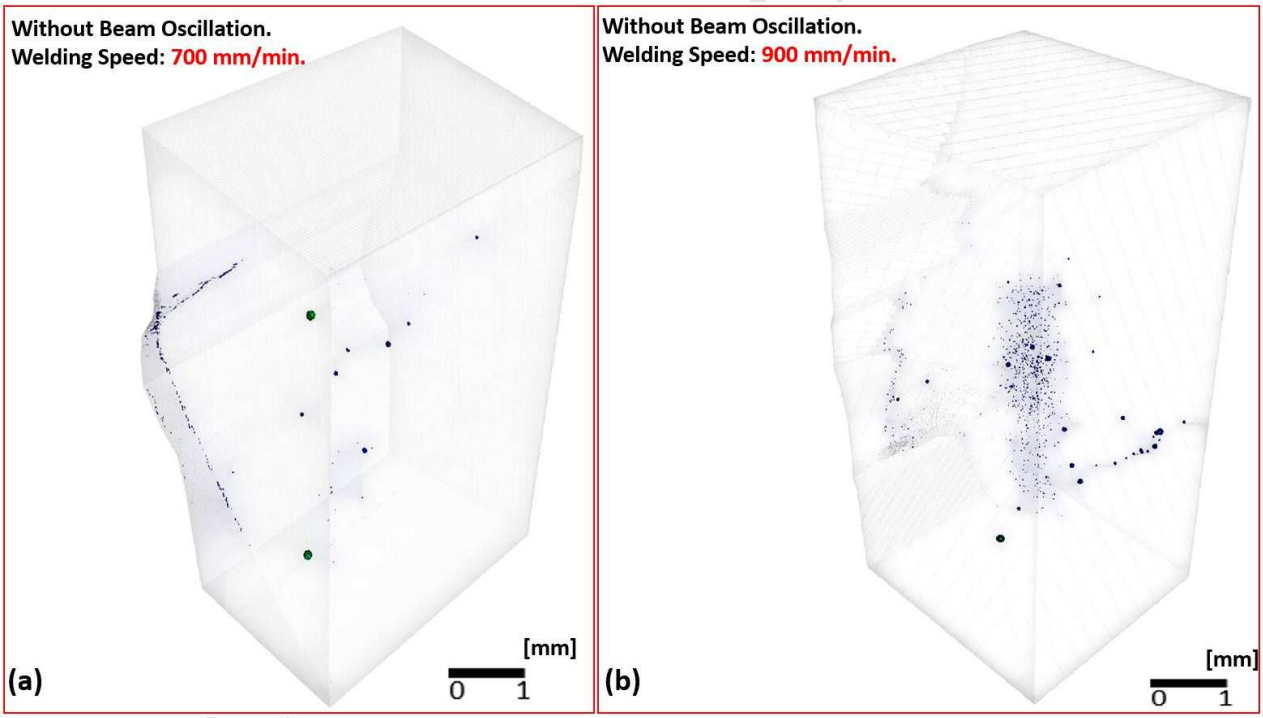

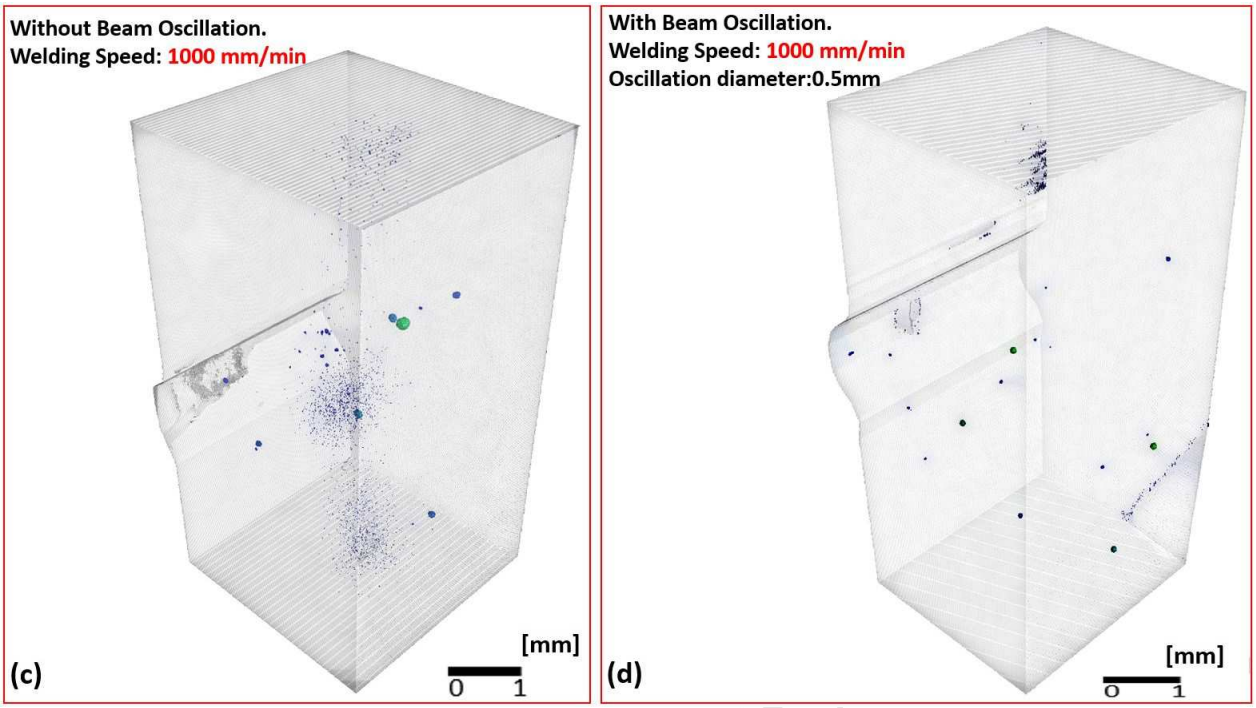

Figure 4: 3D Reconstructed welds with matrix and porosity: (a) Joint 1, (b) Joint 2, (c) Joint 3, and (d) Joint 4 (with oscillation).

XCT data is further analysed and the quantified data of porosity in joints for all weld conditions is shown in Table 6. The average pore size of Joint 1, Joint 2, Joint 3 and joint 4 was found to be 24.9 µm, 21.7 µm, 17.3 µm 15.8 µm respectively. This represents that the application of beam oscillation (joint 4) resulted in small size of pores compared to without beam oscillations. As there is a clear difference between the number of pores produced by the joints and their respective size distributions, comparison between their overall average sizes might not give the complete information. So, the average pore sizes for macro and micro pores were calculated and compared. The average pore size of the macro pores (dia > 75 µm) among all the joints is highest in the joint produced at highest welding speed (1000 mm/min). However, with the application of oscillation beam and maintaining the same welding speed, the average pore size of the macro pores has decreased to 79.6 µm which is found to be the lowest among all the joints. The smallest average pore diameter was observed to be 9.7 µm,

8.5 µm and 8.3 µm in Joint 1, Joint 2, and Joint 3 respectively. But, the minimum pore diameter in Joint 4 (beam oscillation) is decreased to 6.7 µm. The maximum pore diameter is found to be 137.4 µm and 112.6 µm for Joint 1 and Joint 2 respectively. The maximum pore diameter in the case of highest welding speed has increased to 184.7 µm, while it decreased to 87.7 µm in the case of oscillation for Joint 4. The total number of pores has significantly increased as the welding speed increased from Joint 1 to Joint 3. The total number of pores found in Joint 1, Joint 2, and Joint 3 are 295, 779, and 4471 respectively. On the other hand, with beam oscillation condition, in Joint 4 the total number of pores decreased to 161, lowest among all joints. It is also seen that the number of macro pores with diameter greater than 75 µm is least in the oscillation condition of Joint 4 (3 pores), and highest in the Joint 3 (10 pores). Volume of the maximum pore diameter was highest in Joint 3 and lowest in Joint 4 (beam oscillation) i.e., 1.87 x $10^6 \mu m^3$ and 2.23 x $10^5 \mu m^3$ respectively. From the quantified data in Table 6 below, it was evident that the pore density has increased with welding speed from 16 pores /mm^3 in Joint 1 to 46 pores/mm^3 in Joint 2 to 313 pores/mm^3 in Joint 3. However, with the application of beam oscillation in Joint 4 the pore density decreased to 10 pores/mm^3. All the quantified data clearly points out that high welding speed increases the average size and number of pores in the joints. This is due to the fact that there would be very less time for the gas to escape from the surface but enough time to coalescence to form bigger pores. It is also evident that the application of beam oscillation effectively reduced the porosity in the joint 4. This is because the beam oscillation homogenises the weld tract and multiple melting of same spot allows easy escape of gas. Beam oscillation can be perceived as the formation and dissolving of tiny weld pools along the oscillation path with significant overlapping between those tiny pools [25]. In such process a particular location in the weld track undergoes multiple melting that allows dissolved gases to escape. Therefore, chances of porosity formation from dissolved gases diminishes in case of beam oscillation.

Table 6: Quantitative comparison of porosity for all the four welding conditions.

Joint No	Min. Dia. (µm)	Max. Dia. (µm)	Avg. Dia. (µm)	No. of Pores	Average Sphericity	Pores/ mm^3	No's having >75 µm	Avg. Dia. (µm) >75 µm
Joint 1	9.7	137.4	24.9	295	0.78	16	8.0	96.4
Joint 2	8.5	112.6	21.7	779	0.72	46	7.0	95.9
Joint 3	8.3	184.7	17.3	4471	0.75	313	10.0	121.5
Joint 4	6.7	87.7	15.8	161	0.75	10	3.0	79.6

Figure 5 shows the influence of welding speed and beam oscillation on the size and the frequency of pores of all the joints. The percentage of micro pores is found to be more in Joint 3 (high welding speed) and Joint 4 (beam oscillation) both for different reasons. In the case of high speed, the nucleated pores have minimum time to coalescence before the metal around it gets solidified. This resulted in the high percentage of micro pores. In case of beam oscillation an improved churning action lead to a better fluidity in the weld pool making the gas to escape more easily and the pores with less diameter.

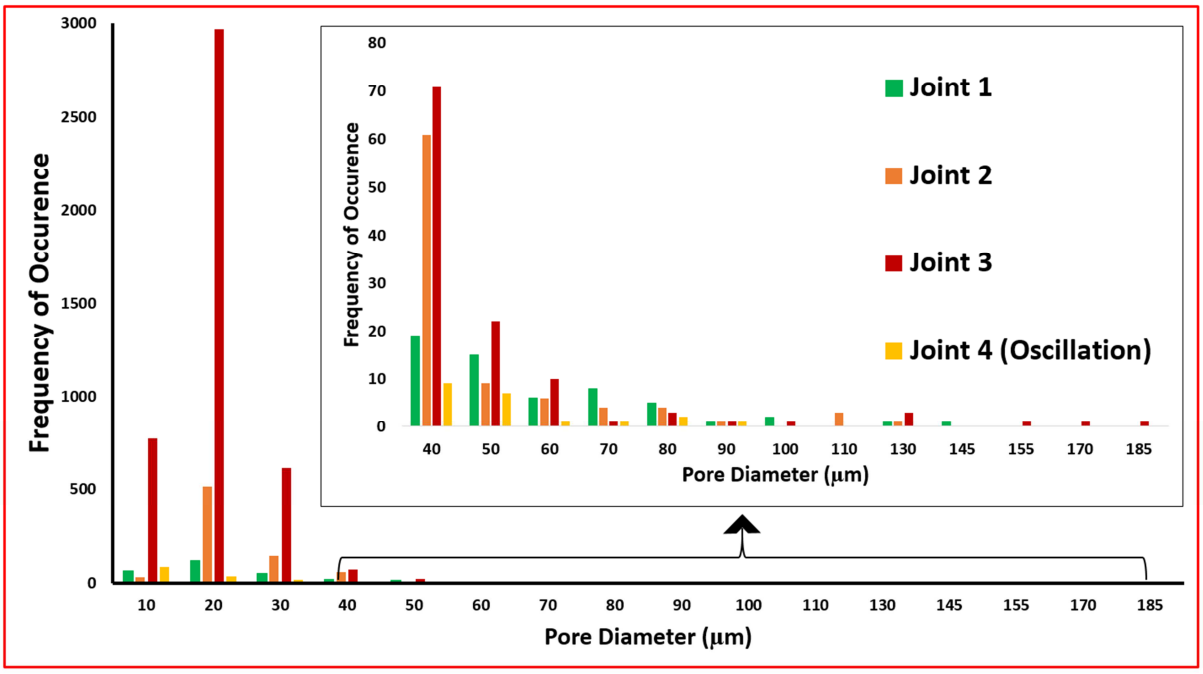

Figure 5: Effect of weld parameters on the size and the frequency of pores.

To have a better understanding of the effect of welding speed and beam oscillation, the largest individual pore in each weld joint is analysed at very high resolution. Largest individual pore morphology of each joint is shown in Figure 6. It can be seen in Figure 6 that the largest individual pore in all the Joints (with and without beam oscillation) are having a smooth spherical morphology. The morphology of the largest pore in the Joint 3 (without beam oscillation, 1000 mm/min) prepared at high welding speed, as shown in Figure 6 (c), has a spherical morphology and highest volume than all the other pores of all the joints. It must also be noted that the Joint 3 has the largest number of micro pores than all the other joints as shown in Figure 4. For better understanding of pores morphology in all joints, sphericity of pores was evaluated using the sphericity formula as shown in Eq. 1.

$$\Psi = \left(\frac{36\,V_p^2}{A_p^3}\right)^{\frac{1}{3}} \quad \text{Eq. 1}$$

Where Ψ is the sphericity, and as Ψ tends to be 1, the pore becomes more spherical in shape. A_p and V_p are the surface area and the volume of the pores respectively. The calculated sphericity of the largest pores of Joint 1, 2, 3 and 4 are 0.54, 0.64, 0.48 and 0.63 respectively.

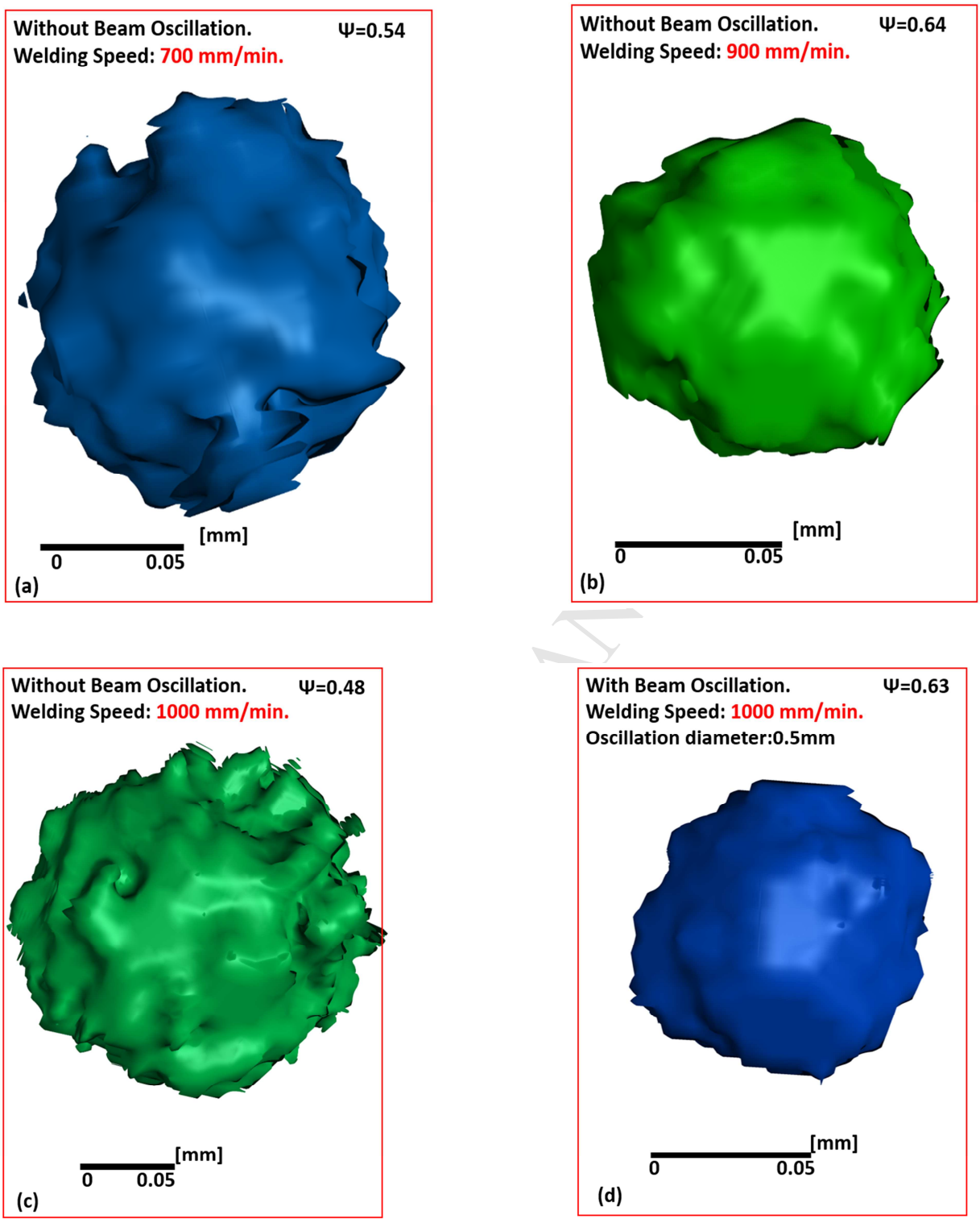

Figure 6: Largest individual pore morphology of (a) Joint 1 (137.4 µm), (b) Joint 2 (112.6 µm), (c) Joint 3 (184.7 µm), and (d) Joint 4 (withoscillation) (87.7 µm).

Sphericity calculation for all the pores in all weld joints was calculated and plotted as shown in Figure 7. The average sphericity of all the micro pores in Joint 1, Joint 2, Joint 3 (highest welding speed), and Joint 4 (oscillation beam) is 0.73, 0.78, 0.75 and 0.79 respectively. It was found that more than 95% of all the micro pores in all the joints with diameter less than 60 µm were having a sphericity value greater 0.6. It was further observed that macro pores with diameter greater than 60 µm have varying sphericity. The percentage of macro pores in Joint 1, Joint 2, Joint 3, and Joint 4 having sphericity greater than 0.6 is 76%, 69%, 8.3%, and 75% respectively. From this observation it is clear that the sphericity of macro pores is very much dependent on the weld parameters and the results also imply that the sphericity of macro pores decrease with welding speed and increases with the application of beam oscillation. Among all the pores in all the joints, pores in joint 3 (highest speed) were found to have lowest sphericity values (as low as 0.38). The percentage of pores with sphericity near to unity is maximum in Joint 4 (with oscillation beam) and minimum in Joint 3 (with highest welding speed). From all the above results, it is evident that irrespective of their size, pore sphericity decreases (especially macro pores) with welding speed and increases with the introduction of beam oscillation. There are three major factors which influence the formation of porosity in the EB-welded joints i.e., keyhole instability, gas entrapment in the weld, and solidification shrinkage in the weld pool. The peculiar mechanism of keyhole instability and its dynamic nature leading to porosity in welds was well discussed by Eriksson et al [26]. Although EBW process is done in high vacuum, gas entrapped in the surfaces of the weld samples can also lead to porosity formation [27]. It is also concluded in literature that the spherical pores with smooth surface morphology (high sphericity) can be formed due to nucleation and growth of gases during solidification in the EBW process [28]. So, the spherical pores formed in the weld joints might be due to the dissolved gases in the weld pool and non-spherical irregular pores with rough surfaces could be formed due to the

solidification shrinkage and keyhole instability in the weld joints. The solidification shrinkage and keyhole instability induced by the fast welding speed and the high cooling rate has increased the percentage of irregular pores in joint 3. Whereas in Joint 4, the beam oscillation not only stabilized the keyhole formation and molten metal flow but also decreased the gas entrapment in the fusion zone. The repeated melting of the same spot during circular beam oscillation allowed most of the gases to escape from the weld pool. As a result of these three factors, very less number of pores are formed and the formed pores have high sphericity in the joint prepared with beam oscillation.

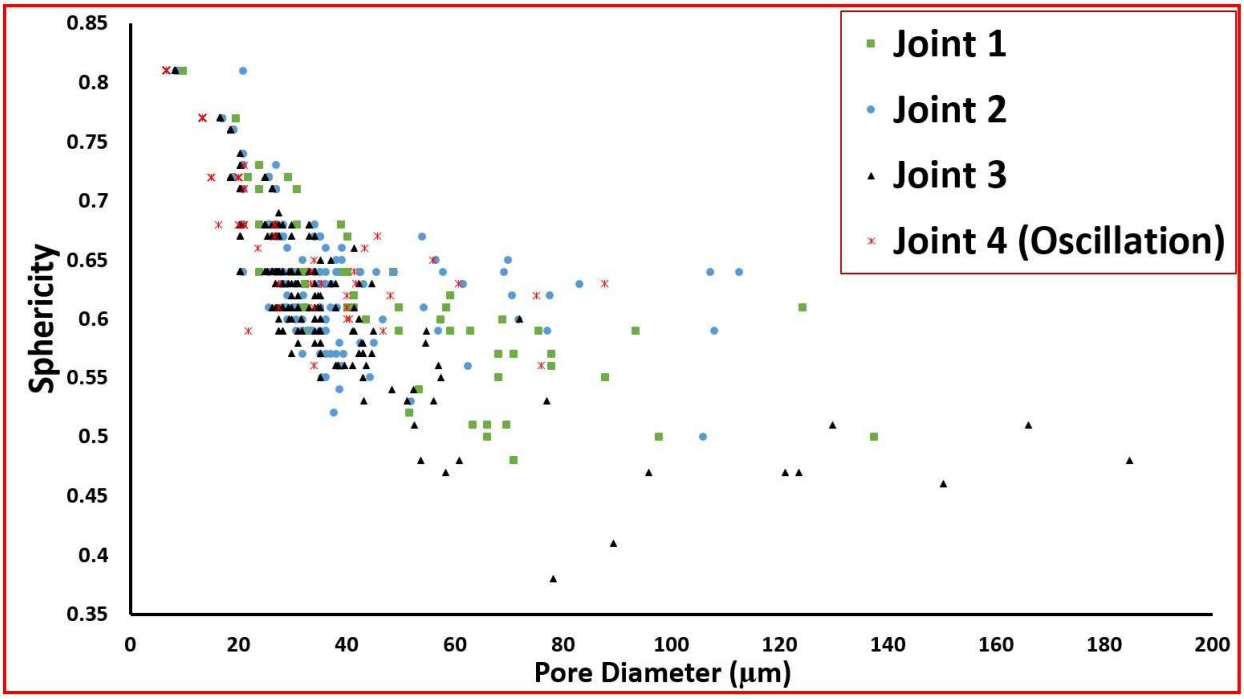

Figure 7: Sphericity variation with respect to the pore diameters of all the joints.

Figure 8 shows the intensity vs Raman shift for all the four joints. For all the four joints, the peak was observed at around 3050 cm^{-1} in the Raman shift representing hydrogen [24]. This can be attributed to the dissolved H_2 in the sample getting trapped due to the high cooling rates in EBW process. It must be noted that the absence of O2 and N2 in the pores is because of the high vacuum in EBW process.

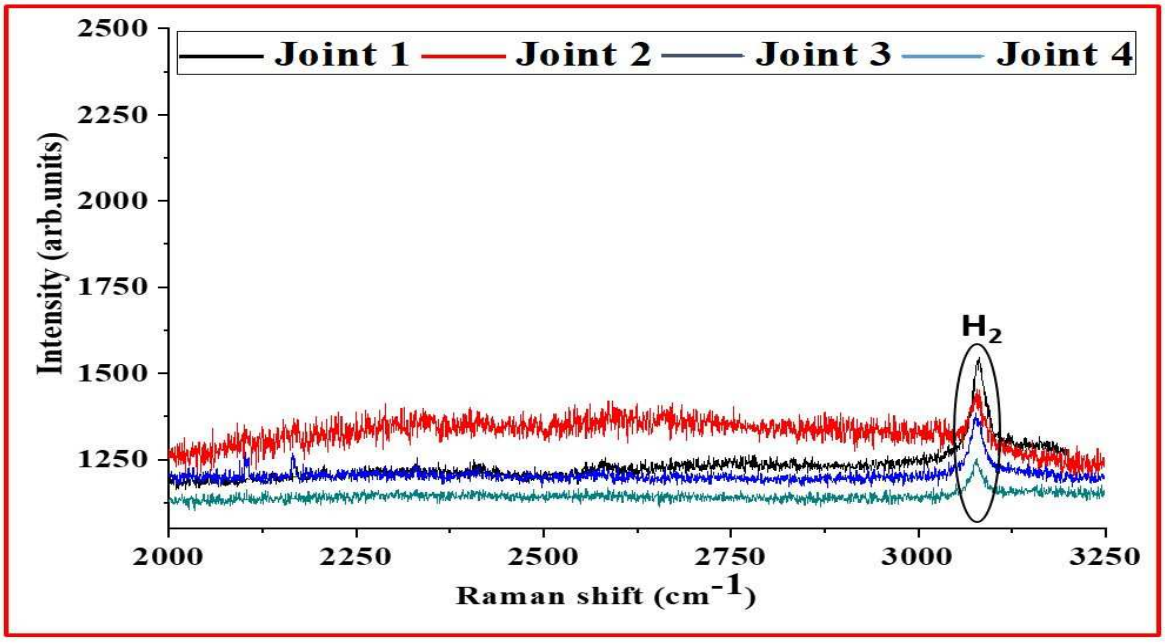

Figure 8: Raman spectroscopy analysis showing H_2 gas in all the joints.

From this work it is understood that size, shape and number of pores formed in the EB-welded Zircaloy-4 joints are very much dependent on the weld parameters. Also, it is evident that the presence of hydrogen gas is the main reason for porosity formation in EBW Zircaloy-4 joints.

4. Conclusions:

- Butt-welding of Zircaloy-4 sheets were successfully carried out using EBW process at four different welding conditions such as without beam oscillation at three different welding speeds and one with beam oscillation at highest speed.
- 3-D porosity images of all the EB-welded joints were successfully captured using X-ray computed tomography (XCT) techniques, analysed and compared among all joints.
- Higher weld speed (1000 mm/min) without beam oscillation resulted in highest percentage of macro pores in weld joints. This is because the higher speed will induce higher cooling rate which consequently decreases the time required for solidification, thereby entrapping more gas pores in the weld.

- Joints prepared with the application of beam oscillation significantly reduced the number of pores which are also small in size compared to all other joints. The repeated melting and solidification coupled by enhanced churning action enabled the gas to escape easily from the weld joint.
- Sphericity calculation shows that the sphericity of pores increases with the decrease of their respective sizes thereby indicating small size gas pores.
- Raman spectroscopy confirmed the presence of Hydrogen gas in the pores of all the joints.
- It was clear from this study that the application of beam oscillation results in quality weld products by decreasing the porosity formation.

5. Acknowledgements

The authors are greatly thankful to the Nuclear Fuel Complex, Hyderabad for supplying Zircaloy-4 sheets. The authors also thank to Board of Research for Nuclear Science (BRNS) for financial assistance to carry out the work. The authors also acknowledge Bhabha Atomic Research Centre (BARC) for donating the EBW machine to IIT Kharagpur, India.

6. References

[1]. M. Ahmad, J.. Akhter, M.. Shaikh, M. Akhtar, M. Iqbal, M.. Chaudhry, Hardness and microstructural studies of electron beam welded joints of Zircaloy-4 and stainless steel, J. Nucl. Mater. 301 (2002) 118–121. doi:10.1016/S0022-3115(01)00757-7.

[2]. A. Ravi Shankar, V.R. Raju, M. Narayana Rao, U. Kamachi Mudali, H.S. Khatak, B. Raj, Corrosion of Zircaloy-4 and its welds in nitric acid medium, Corros. Sci. 49 (2007) 3527–3538. doi:10.1016/j.corsci.2007.03.029.

[3]. J.B. Bai, C. Prioul, S. Lansiart, D. François, Brittle fracture induced by hydrides in zircaloy-4, Scr. Metall. Mater. 25 (1991) 2559–2563. doi:10.1016/0956-716X(91)90068-C.

[4]. K. Bhanumurthy, J. Krishnan, G.B. Kale, S. Banerjee, Transition joints between Zircaloy-2 and stainless steel by diffusion bonding, J. Nucl. Mater. 217 (1994) 67–74. doi:10.1016/0022-3115(94)90305-0.

[5]. P.D. Wilson (Ed.), The Nuclear Fuel Cycle: From Ore to Wastes, Oxford University Press, Oxford (1996).

[6]. N.A.P. Kiran Kumar, J.A. Szpunar, Z. He, Microstructural studies and crystallographic orientation of different zones and δ-hydrides in resistance welded Zircaloy-4 sheets, J. Nucl. Mater. 414 (2011) 341–351. doi:10.1016/j.jnucmat.2011.03.027.

[7]. K. Song, Laser Welding Unit for Intersection Line Welding of Spacer Grid Inner Straps and its Application, J. Laser Micro/Nanoengineering. 4 (2009) 11–17. doi:10.2961/jlmn.2009.01.0003.

[8]. K. Song, Determination of the Optimum Welding Parameters for a Laser Welded Spacer Grid Assembly for PWRs, J. Laser Micro/Nanoengineering. 2 (2007) 95–99. doi:10.2961/jlmn.2007.01.0017.

[9]. K.N. Song, S.B. Lee, M.B. Lee, M.K. Shin, J.J. Lee, New Spacer Grid to Enhance Mechanical/Structural Performance, J. Nucl. Sci. Technol. 47 (2010) 295–303. doi:10.1080/18811248.2010.9711957.

[10].M.S. Węglowski, S. Błacha, A. Phillips, Electron beam welding - Techniques and trends - Review, Vacuum. 130 (2016) 72–92. doi:10.1016/j.vacuum.2016.05.004.

[11]. K. Devendranath Ramkumar, R. Sridhar, S. Periwal, S. Oza, V. Saxena, P. Hidad, N. Arivazhagan, Investigations on the structure – Property relationships of electron beam welded

Inconel 625 and UNS 32205, Mater. Des. 68 (2015) 158–166. doi:10.1016/j.matdes.2014.12.032.

[12]. S.K. Dinda, M. Basiruddin Sk, G.G. Roy, P. Srirangam, Microstructure and mechanical properties of electron beam welded dissimilar steel to Fe–Al alloy joints, Mater. Sci. Eng. A. 677 (2016) 182–192. doi:10.1016/j.msea.2016.09.050.

[13]. S. Kou, A criterion for cracking during solidification, Acta Mater. 88 (2015) 366–374. doi:10.1016/j.actamat.2015.01.034.

[14]. I. Valavanis, D. Kosmopoulos, Multiclass defect detection and classification in weld radiographic images using geometric and texture features, Expert Syst. Appl. 37 (2010) 7606–7614. doi:10.1016/j.eswa.2010.04.082.

[15]. H. Park, M. Choi, J. Park, W. Kim, A study on detection of micro-cracks in the dissimilar metal weld through ultrasound infrared thermography, Infrared Phys. Technol. 62 (2014) 124–131. doi:10.1016/j.infrared.2013.10.006.

[16]. T. Yuan, X. Chai, Z. Luo, S. Kou, Predicting susceptibility of magnesium alloys to weld-edge cracking, Acta Mater. 90 (2015) 242–251. doi:10.1016/j.actamat.2015.02.031.

[17]. S.K. Dinda, J.M. Warnett, M.A. Williams, G.G. Roy, P. Srirangam, 3D imaging and quantification of porosity in electron beam welded dissimilar steel to Fe-Al alloy joints by X-ray tomography, Mater. Des. 96 (2016) 224–231. doi:10.1016/j.matdes.2016.02.010.

[18]. T. Mohandas, D. Banerjee, V. V. Kutumba Rao, Fusion zone microstructure and porosity in electron beam welds of an α+β titanium alloy, Metall. Mater. Trans. A. 30 (1999) 789–798. doi:10.1007/s11661-999-0071-3.

[19]. C.J. Parga, I.J. van Rooyen, B.D. Coryell, W.R. Lloyd, L.N. Valenti, H. Usman, Room temperature mechanical properties of electron beam welded zircaloy-4 sheet, J. Mater. Process. Technol. 241 (2017) 73–85. doi:10.1016/j.jmatprotec.2016.11.001.

[20]. P. Mishra, V.P. Jathar, J.L. Singh, D.N. Sah, P.K. Shah, S. Anantharaman, In-reactor degradation of fuel and cladding in fuel pins operated with weld defects, in: J. Nucl. Mater., 2013: pp. 217–223. doi:10.1016/j.jnucmat.2012.05.033.

[21]. W. Tao, C. Cai, L. Li, Y. Chen, Y.L. Wang, Pulsed laser spot welding of intersection points for Zircaloy-4 spacer grid assembly, Mater. Des. 52 (2013) 487–494. doi:10.1016/j.matdes.2013.05.037.

[22]. R. Nomoto, Y. Takayama, F. Tsuchida, H. Nakajima, Non-destructive three-dimensional evaluation of pores at different welded joints and their effects on joints strength, Dent. Mater. 26 (2010). doi:10.1016/j.dental.2010.08.006.

[23]. J. Kar, S.K. Dinda, G.G. Roy, S.K. Roy, P. Srirangam, X-ray tomography study on porosity in electron beam welded dissimilar copper–304SS joints, Vacuum. 149 (2018) 200–206. doi:10.1016/j.vacuum.2017.12.038.

[24]. A. Leitch, V. Alex, J. Weber, Raman Spectroscopy of Hydrogen Molecules in Crystalline Silicon, Phys. Rev. Lett. 81 (1998) 421–424. doi:10.1103/PhysRevLett.81.421.

[25]. J. Kar, S.K. Roy, G.G. Roy, Effect of beam oscillation on electron beam welding of copper with AISI-304 stainless steel, J. Mater. Process. Technol. 233 (2016) 174–185. doi:10.1016/j.jmatprotec.2016.03.001.

[26]. I. Eriksson, J. Powell, A.F.H. Kaplan, Melt behavior on the keyhole front during high speed laser welding, Opt. Lasers Eng. 51 (2013) 735–740. doi:10.1016/j.optlaseng.2013.01.008.

[27]. P. Fu, Z. Mao, C. Zuo, Y. Wang, C. Wang, Microstructures and fatigue properties of electron beam welds with beam oscillation for heavy section TC4-DT alloy, Chinese J. Aeronaut. 27 (2014) 1015–1021. doi:10.1016/j.cja.2014.03.020.

[28]. J.L. Huang, N. Warnken, J.C. Gebelin, M. Strangwood, R.C. Reed, On the mechanism of porosity formation during welding of titanium alloys, Acta Mater. 60 (2012) 3215–3225. doi:10.1016/j.actamat.2012.02.035.

Highlights

- Electron Beam Welding of Zircaloy-4 was successfully carried out for four different welding parameters such as with beam oscillation, without beam oscillation and at different welding speeds.
- XCT technique was used to analyse the 3D porosity: The average size, number and shape of the pores in the Electron Beam welded joints of Zircaloy-4.
- Weld porosity increased substantially with the increase in weld speed.
- Results show that the application of beam oscillation resulted in smaller average pore size and lesser number of pores compared to without beam oscillation condition